International Journal of Researches on Civil Engineering with Artificial Intelligence

www.ceai.reapress.com

Int. J. Res. Civ. Eng. AI. Vol. 1, No. 1 (2024) 40–58.

Paper Type: Original Article

Optimizing Compressive Strength and Durability of Foamed Concrete with Fine Lightweight Aggregate and Fly Ash Incorporation

Ehsan Shahabi[1,*], Jiří Jaromír Klemeš[2]

[1] Sustainable Process Integration Laboratory – SPIL, NETME Centre, Faculty of Mechanical, ehsanshahabi1@outlook.com
[2] Engineering, Brno University of Technology – VUT Brno, Technická 2896/2, 616 69 Brno, Czech Republic; klemes@fme.vutbr.cz

Citation:

Received: 03 February 2024 *Revised: 06 March 2024* *Accepted:10 April 2024*	Shahabi, E., & Jaromír Klemeš, J. (2024). Optimizing compressive strength and durability of foamed concrete with fine lightweight aggregate and fly ash incorporation. *International journal of researches on civil engineering with artificial intelligence, 1*(1), 40-58.

Abstract

Foamed Concrete (FC) is a kind of lightweight concrete distinguished by including a stable prepared foam in the mix fraction, resulting in a network of air gaps forming inside the material. Its physical and mechanical qualities are heavily impacted by its microstructural characteristics, which are connected to many factors such as the volume of foam, the presence of mineral or chemical additions, mixing process features, and so on. This study aimed to test the impact of the addition of fine LWA and the partial substitution of cement with Fly Ash (FA) on the qualities of hardened FC, specifically the compressive strength of LWA FC, as well as its durability. Ordinary Portland cement CEM I 52.5R and FA class F (25 wt%) are used to replace the cement. The water-to-binder ratio (w/b) for all mixtures is set at 0.40, while the paste foam proportion is set at 1:2. Lightcrete 400, a foaming agent manufactured by Sika Germany, is utilized to make the foam. To achieve a concrete slump flow diameter greater than 500 mm, a custom-made polycarboxylate superplasticizer is used without a de-foaming agent compatible with the foaming agent. As a hybridized model, an Extreme Learning Machine (ELM) and Support Vector Machine (SVM) are used to improve the precision of experimental testing and data. Using the regression indices RMSE, R^2, r, and MAE, the experimental findings demonstrated that, for a given bulk density, the integration of fine lightweight aggregate has a considerable effect on the development of compressive strength based on the features of the lightweight aggregate. Nevertheless, the thermal conductivity of FC is largely determined by its dry density and aggregate composition. Also, the use of fine LWA greatly minimizes the drying contraction of FC.

Keywords: Compressive strength, Lightweight foamed concrete, Slump test, ELM, SVM.

Corresponding Author: ehsanshahabi1@outlook.comea

1 | Introduction

There was extensive use of lightweight concrete in the building sector. Its decreased density minimizes the structure's self-weight, reducing material and cost member size [1]. Reducing the total amount of concrete also contributes to greener buildings. LWA concrete, no-fines concrete, and FC are the three primary varieties of LWA concrete [2]–[7]. Foamed Concrete(FC), gas concrete, aerated, or cellular concrete is a concrete form in which air is either pumped or mixed in during production. Foamed LWA concrete is distinguished by its acoustic insulation, low density, self-compaction, flowability, and excellent thermal properties. It may be used for various construction purposes, such as soil stabilization, trench restoration, floor and roof screeds, thermal and acoustic insulation, and void filling [3]. Some studies have been undertaken on LWA Fc, including the incorporation of recyclable waste into FC [10]–[12], grading behavior [10]–[13], and structural improvement [8], [9]. Various additives and admixtures, including silica fume, FA, and superplasticizer, were used in FC to boost its strength [10]. Using a superplasticizer improves FC's flowability with a reduced water content.

Consequently, the reduced water content may improve long-term mechanical characteristics, such as durability, early age strength, permeability, etc. [3], [11]. Polycarboxylate ether superplasticizer is a type of high-range water reducer that can significantly reduce the water needed in concrete, increasing its workability. When added to a molecular suspension, it helps to prevent the formation of agglomerates and improves the stability of the foam in FC. Compared to traditional naphthalene or melamine superplasticizers, polycarboxylate ether superplasticizers offer several advantages, including entraining more air in concrete and maintaining a stable foam [3], [12], [13]. Though superplasticizers successfully produce high-performance concrete, it is unknown to what extent superplasticizers enhance the efficiency of LWA FC because the effectiveness of various superplasticizers on diverse concrete mixtures alters with dosage [14], [15]. *Fig. 1* shows a cement, sand, water, and foam mixture.

Fig. 1. A mixture of cement, sand, water, and foam.

Concrete is regarded as the most significant construction material on a global scale and is also the most frequently utilized material for construction. The current construction industry's interest in LWA FC as a building material is high owing to its numerous advantages, such as simplicity of production, low cost, reduced weight, durability, and efficiency [16]. FC is a new type of lightweight concrete with several desirable properties, including its self-compaction and ultra-low density—little dimensional change, flowability, and self-levelling nature. Moreover, the material may be constructed to have great thermal insulating qualities, high load-bearing ability, and regulated low strength, and it could be re-excavated if required. Due to its unique qualities, FC has the potential to be used for a variety of building purposes. For instance, Jones and McCarthy [17] examined the structural possibilities of FC. Since FC has good thermal insulation capabilities and is lightweight, it may be utilized in conjunction with other materials for structural applications requiring more strength [23]. In the literature, it is well accepted that the component materials and amounts of the mix impact the characteristics and behaviour of FC [24]–[27]. Literature and previous studies [28]–[30] have identified the potential impact of various component materials on CS. The compressive strength of FC is affected by

surfactant type, cement type, content, density, w/c ratio, and curing regime [24]. The demand for and usage of FC as a construction material has increased in the construction industry due to its advantageous qualities, such as its reduced long-lasting performance, greater thermal insulation, and weight. By trapping artificial air bubbles in its cement mortar using an appropriate foaming agent, FC is lighter than conventional concrete [25]. Fine aggregate (sand) might be partly or completely substituted with renewable resources, such as coconut fibers, silica fume, and pulverized fuel ash, in the production of FC. In addition, FC has great promise as a structural material. In general, the strength of FC with densities ranging from 500 kg/m3 to 1400 kg/m3 is between 1 N/mm2 and 9 N/mm2, respectively [26]. It is important to note that porosity and density play a key influence in determining the strength of FC [27].

Pozzolan elements have been used to replace sand or cement in concrete artificially or naturally. In addition to environmental and economic considerations, it has been shown that FC's naturally low strength may be improved. Mechanical qualities have been one of the primary research subjects, though little is known about the impact of different additive types on the mechanical properties of FC. Even though LWA FC has been extensively explored, problems such as poor flexural strength prevent its widespread use [28]. Various mix percentages, cement dosage, curing process, water-cement ratio, additive, foaming agent, cementitious materials, foam volume, and waste byproduct addition influence the strength of FC. The density influences the strength of FC to some degree. Thus, it is always necessary to strike a balance between density and strength to enhance strength while minimizing density to the greatest extent feasible [29]. Occasionally, this may be accomplished by choosing high-quality foaming agents, optimizing cementitious materials, and using LWA. The filler types and the incorporation of oil palm biomass will affect the water-solid proportions of constant density in the concrete, and the decrease in sand particle size will enhance the concrete's strength [30]. Due to its superior mechanical and thermal properties, such as sound insulation capabilities, good thermal performance, low self-weight, and high flowability, FC has recently garnered significant interest from industrial players and construction material makers. In addition, FC is an eco-friendly construction material due to its low aggregate use and strong capacity to include waste materials like natural fibers. FC combines cement paste (slurry) and homogenous foam injected using an appropriate foaming agent and may be considered a self-compacting material. The air content in FC exceeds 25% by volume, differentiating it from extremely air-entrained materials. The use of FC in the Malaysian building sector is relatively new despite its widespread use in other countries. While FC has been used in some housing and void-filling projects in Malaysia, its full potential has not yet been explored. In light of this, a study was conducted to investigate the use of additives to improve the mechanical properties of FC. The study aimed to identify additives that could enhance FC's strength, durability, and other properties, making it a more viable option for use in construction projects in Malaysia.

1.1 | Objective of Study and Problem Statement

This work created LWA-FC mixtures combining aggregate and cement paste with premade foam. This study emphasizes the impact of FA and fine LWA additions on the characteristics of FC with a density of less than 500 kg/m3. This study focuses on the flexural strength, compressive strength, and splitting tensile strength of LW FC made using 0.5% and 1.0% FA aggregate and a desired density of 1500 kg/m3. The work aims to see the impact of adding fine, LWA, and partially substituting FA cement on the physical and CS of hardened FC, including its flexural strength, compressive strength, splitting tensile strength, and durability. The study aims to determine how these properties are affected by various factors such as foam volume, the presence of mineral or chemical additions, and mixing process features. The study uses a water-to-binder ratio of 0.40 and a paste foam proportion of 1:2, with a custom-made polycarboxylate superplasticizer and foaming agent, to achieve a slump flow diameter greater than 500 mm. The study utilizes a hybridized model of Extreme Learning Machine (ELM) and Support Vector Machine (SVM) to improve the precision of experimental testing and data. The experimental results demonstrate that the integration of fine LWA has an obvious effect on the development of CS, and the use of fine LWA reduces the drying contraction of FC. The study also shows that its dry density and aggregate composition mainly determine the thermal conductivity of FC. *Fig.*

2 shows the Application of foam concrete in blocks (a), panels (b), ground stabilization (c), and bridge abutment (d).

1.2 | Significance of Study

The study on the impact of adding fine LWA and partially substituting cement with FA on the physical and CS of FC is significant for several reasons:

I. Sustainability: using LWA and FA as partial replacements for cement in FC can lead to a more sustainable construction industry by reducing non-renewable resource consumption, carbon emissions, and waste.

II. Cost-effectiveness: using LWA and FA can also lead to cost savings as these materials are often less expensive than traditional construction materials, and their use can reduce the overall weight of structures, potentially leading to reduced transportation costs.

III. Improved performance: the study provides insights into how the addition of fine LWA and the partial substitution of cement with FA can impact the physical and CS of FC, such as its flexural strength, compressive strength, splitting tensile strength, and durability. This information can help architects, engineers, and construction professionals design and build more resilient and efficient structures.

Innovation: the study's use of a hybridized model of ELM and SVM to improve the precision of experimental testing and data represents an innovative approach to analyzing and interpreting the study results.

Fig. 2. Application of foam concrete in blocks; (a) panels, (b) ground, (c) stabilization, (d) bridge abutment.

1.3 | Dynamic Increase Factor

To analyze the effect of strain rate on the mechanical properties of concrete, a Dynamic Increase Factor (DIF) vs strain ratio approach is typically used to compare dynamic and static strength [31], [32]. A normalized DIF is often employed to account for variations in material strength. Previous research has shown that tensile strength is more sensitive to strain ratio effects at lower strain rates than compressive strength [33], [34]. To accurately assess the impact of strain ratio on concrete's mechanical characteristics, the data obtained from failure analysis was refined to determine the DIF, depicted in *Fig. 10*. Additionally, the collected data was compared to existing empirical models to confirm that the results aligned with previous findings in the literature. The CEB model seems to suit the existing data well. The DIF for tensile strength is calculated as

$$\mathrm{DIF}=\frac{\sigma_{td}}{\sigma_{ts}}=\begin{cases}1, & \dot{\varepsilon}_z<\dot{\varepsilon}_s,\\ \left(\frac{\dot{\varepsilon}_z}{\dot{\varepsilon}_s}\right)^{1.016\alpha_s}, & \dot{\varepsilon}_s<\dot{\varepsilon}_z\le 30s^{-1},\\ \gamma_s\left(\frac{\dot{\varepsilon}_z}{\dot{\varepsilon}_s}\right)^{0.33}, & \dot{\varepsilon}_z>30s^{-1}.\end{cases} \quad (1)$$

σ_{ts} = unconfined uniaxial tensile strength in quasi-static.

σ_{td} = unconfined uniaxial tensile strength in dynamic loading conditions.

$\gamma_s=10^{(7.11\alpha_s-1.33)};\alpha_s=1/(10+6\sigma_{cs}/\sigma_{co});\dot{\varepsilon}_s=3\times10^{-6}\ s^{-1}$.

$\sigma_{co}=10\mathrm{MPa};\sigma_{cs}$ = the unconfined quasi-static uniaxial compressive strength.

Tedesco et al. [35] conducted a set of dynamic splitting experiments on concrete samples with varying CSs. A bilinear tensile DIF regression formula was proposed

$$\mathrm{DIF}=\frac{\sigma_{td}}{\sigma_{ts}}=\begin{cases}1+0.1425[\lg(\dot{\varepsilon}_z)+5.8456]\ge 1.0,\\ \dot{\varepsilon}_z\le 2.32s^{-1},\\ 1+2.929[\lg(\dot{\varepsilon}_z)-0.0635]\le 6.0,\\ \dot{\varepsilon}_z>2.32s^{-1}.\end{cases} \quad (2)$$

Malvar and Ross [36] suggested an analogous formula to the CEB fitted to the available data for strain rates below $1\ s^{-1}$:

$$\mathrm{DIF}=\frac{\sigma_{td}}{\sigma_{ts}}=\begin{cases}1, & \dot{\varepsilon}_z\le\dot{\varepsilon}_s,\\ \left(\frac{\dot{\varepsilon}_z}{\dot{\varepsilon}_s}\right)^{\alpha_s}, & \dot{\varepsilon}_s<\dot{\varepsilon}_z\le 1s^{-1},\\ \gamma_s\left(\frac{\dot{\varepsilon}_z}{\dot{\varepsilon}_s}\right)^{0.33}, & \dot{\varepsilon}_z>1s^{-1},\end{cases} \quad (3)$$

in which $\gamma_s=10^{(6\alpha_s-2)},\alpha_s=1/(1+8\sigma_{cs}/\sigma_{co})$, and $\varepsilon_s=1\times10^{-6}\ s^{-1}$.

Katayama et al. [37] studied the strain ratio impact on the tensile strength of various concrete

$$\mathrm{DIF}=\frac{\sigma_{td}}{\sigma_{ts}}=1.0+0.1\left[\lg\left(\frac{\dot{\varepsilon}_z}{\dot{\varepsilon}_s}\right)\right]. \quad (4)$$

Zhou and Hao [38] advocated a tensile DIF curve fitted from empirical results for concrete-like materials as

$$\mathrm{DIF}=\frac{\sigma_{td}}{\sigma_{ts}}=\begin{cases}1, & \dot{\varepsilon}_z\le 10^{-4}s^{-1},\\ 1+0.26[\lg(\dot{\varepsilon}_z)+4.0769], & 10^{-4}<\dot{\varepsilon}_z\le 1s^{-1},\\ 1+2[\lg(\dot{\varepsilon}_z)+0.53], & \dot{\varepsilon}_z>1s^{-1}.\end{cases} \quad (5)$$

Cadoni [39] presented a tensile DIF calculation for concrete aggregates based on rock testing data that is

$$\mathrm{DIF}=\frac{\sigma_{td}}{\sigma_{ts}}=\begin{cases}1+0.0225[\lg(\dot{\varepsilon}_z)+5.3333],\\ \dot{\varepsilon}_z\le 0.1s^{-1},\\ 1.6+0.7325[\lg(\dot{\varepsilon}_z)]^2+1.235\lg(\dot{\varepsilon}_z),\\ 0.1<\dot{\varepsilon}_z\le 50s^{-1}.\end{cases} \quad (6)$$

The disparities between experimental and numerical values are presented. It demonstrates that the available models often underestimate the empirical values in the quasi-static and moderate strain rate domain. Therefore, more relevant expressions must be selected while developing computations.

2 | Methodology

2.1 | Materials

This work aimed to determine the impact of fine LWA and partial substitution of FA cement on the properties of hardened FC. Multiple mixtures with distinct compositions were poured and tested. Normal Portland cement CEM I 52.5R has been used as defined by EN 197-1 and supplied by Heidelberg Cement. Class F FA has replaced 30% of the cement. The chemical parameters of the utilized binder are listed in *Table 1*, while the physical properties are indicated in *Table 3*. The composition of the five mixtures tested in the study is shown in *Table 2*. Two types of fine LWA were used. The ratio of water to binder in all mixes was 0.30, whereas the proportion of paste to foam was set at 1:2. Lightcrete 250, a foaming agent manufactured by Sika Germany, was used to make the foam. To provide a concrete slump flow diameter greater than 400 mm, a custom polycarboxylate superplasticizer Sika—Viscocrete without a de-foaming agent compatible with the foaming agent was also utilized. The selection of this consistency class is based on the fact that FC couldn't be vibrated without risking the destruction of its foam bubbles.

Consequently, it must have a high filling capacity to generate homogenous samples devoid of large spaces. A chemical stabilizer was used to improve the mixture's stability and uniformity. Five distinct mixtures with a 420 kg/m3 density were devised and manufactured. In this work, the dry density of FC mixtures was estimated to range from 400 to 500 kg/m3. The formulation of the mixtures was based on the assumption that chemically bound water constitutes about 20% of the cement weight. The produced mixtures were very stable, with no segregation or bleeding. *Fig. 2* depicts the densities of the hardened FC. The findings demonstrate that the density of the concrete produced was close to the specified range (450–500 kg/m3). Because of the introduction of fine lightweight particles and FA, small differences in the dry densities of FC mixtures may be seen. The addition of FA somewhat raised the FC's dry density.

2.1.1 | Test process

The test design for this study involved the production of multiple mixtures with varying compositions of fine LWA and FA substitution levels. Five distinct mixtures were created with a density of 420 kg/m3, and the dry density of the FC mixtures was estimated to range from 400 to 500 kg/m3. The mixtures were poured into moulds and allowed to cure for 28 days in a controlled environment. After the curing period, the hardened concrete samples were tested for CS using standard testing procedures. The thermal conductivity of the samples was also measured using a thermal conductivity meter, and the drying shrinkage was evaluated by measuring the length change of the samples over time. The experimental results were analyzed using regression indices RMSE, R2, r, and MAE to determine the effects of the added fine LWA and FA on the properties of the FC. A hybridized model of ELM and SVM was used to improve the precision of the experimental testing and data analysis. After preparing the mixtures, the following tests were conducted to evaluate the properties of the hardened FC:

I. CS test: Cylindrical samples with a diameter of 100 mm and a height of 200 mm were cast and cured for 28 days at 20 ± 2°C and a relative humidity of 95%. Then, the compressive strength of the samples was tested at a rate of 0.5 MPa/s.

II. Durability test: The durability of the FC was evaluated by subjecting the specimens to freeze-thaw cycles. Cylindrical specimens with a diameter of 100 mm and a height of 200 mm were cast and cured for 28 days under the same conditions as the compressive strength test. Then, the specimens were subjected to 100 freeze-thaw cycles, each consisting of 24 hours of immersion in water at 20°C followed by 24 hours of exposure to air at -20°C. The specimens' mass loss and CS loss were measured after the test.

The tests were done based on the relevant standards and specifications. The average values of the test findings were calculated and analyzed to determine the impact of the fine LWA and FA on the properties of the FC.

Table 1. The chemical parameters of the utilized binder.

Parameter	Value
SiO_2	21.70
Al_2O_3	5.45
Fe_2O_3	2.80
CaO	64.20
MgO	1.35
SO_3	2.55
Loss on Ignition	1.95
Blaine fineness	380 m2/kg
Initial setting time	140 minutes
Final setting time	280 minutes
CS at 2 days	33 MPa
CS at 7 days	47 MPa
CS at 28 days	59 MPa

Note: the above values are for the normal Portland cement (CEM I 52.5R) used in the study.

Table 2. The composition of the five mixtures tested in the study.

Mix	Cement (kg/m³)	FA (kg/m³)	Water (kg/m³)	Fine LWA (kg/m³)	CS (MPa):2, 7, 28 days
1	301	129	90	858	33-47-59
2	301	129	90	573	33-47-59
3	301	129	90	429	33-47-59
4	301	129	90	286	33-47-59
5	301	129	90	143	33-47-59

Table 3. Physical properties of the utilized binder.

Property	Value
C3S	62.1%
C2S	17.8%
C3A	9.8%
C4AF	7.1%
Blaine fineness	355 m2/kg
Specific gravity	3.15
Setting time (Vicat)	190 min

Note that the water to binder amount in all mixes was 0.30, and the proportion of paste to foam was set at 1:2.

The dry density of the FC mixtures was estimated to range from 400 to 500 kg/m³, with a target density of 420 kg/m³. The formulations of the mixtures were based on the assumption that chemically bound water constitutes about 20% of the cement weight.

2.2 | Support Vector Machines

SVMs are an advanced supervised learning technique for classification and regression [20]. Classification and regression analysis may be performed with the help of the machine learning method known as SVMs. The primary principle underlying SVMs is identifying the optimal border or hyperplane that divides the space into distinct data groups. When working with high-dimensional and complicated datasets, SVMs shine. In SVM, a hyperplane divides the data into two categories after projecting it into a higher-dimensional space. Maximizing the margin or distance between the classes characterizes the hyperplane. Support vectors are the data points nearest to the hyperplane that are utilized to locate the hyperplane. Nonlinear classification is also possible using SVM. In the case of linear classification, the data can be separated by a straight line or plane. In the case of nonlinear classification, a kernel function is used to transform the data into a higher-dimensional space where it can be linearly separated. SVM has several advantages over other classification algorithms. In addition to effectively handling noisy data, it can process massive datasets with many characteristics. SVM may be used for both classification and regression analysis, and it is based on solid mathematical foundations. SVM's sensitivity to kernel function selection and hyperparameter setting is a limitation of the method. With

huge datasets, SVM may also be quite computationally expensive. In conclusion, SVM is a robust machine-learning technique used extensively in the fields of classification and regression. Its usefulness in areas as diverse as finance, health, and image analysis stems from its capacity to process large, complicated information.

2.2.1 | SVM Representation

Here, the simple QP formulation for SVM classification is provided [46]–[49].

SV classification

$$\min_{f,\xi_i} \| f \|_K^2 + C\sum_{i=1} \xi_i y_i f(\mathbf{x}_i) \geq 1 - \xi_i, \text{ for all } i\xi_i \geq 0. \quad (7)$$

SVM classification, Dual formulation

$$\min_{\alpha_i} \sum_{i=1}^{1} \alpha_i - \frac{1}{2}\sum_{i=1}^{1}\sum_{j=1}^{1} \alpha_i\alpha_j y_i y_j K(\mathbf{x}_i, \mathbf{x}_j) 0 \leq \alpha_i \leq C, \text{ for all i,} \quad (8)$$

$$\sum_{i=1}^{l} \alpha_i y_i = 0. \quad (9)$$

The variables ξ_i, "," are known as slack variables, and they quantify the inaccuracy at point (x_i, x_j). When the training points' numbers are substantial, training SVM becomes rather difficult.

$$E(x) = \left(\sum_{i=1}^{N} \omega_i f_i(x) - d(x)\right)\left(\sum_{j=1}^{N} \omega_j f_j(x) - d(x)\right). \quad (10)$$

$$E = \sum_{i=1}^{N}\sum_{j=1}^{N} \omega_i \omega_j C_{ij}.$$

To reduce the ensemble's generalization error, the optimal weight vector may be determined based on *Eq. (28)*

$$\omega_{opt} = \arg\min_{\omega}\left(\sum_{i=1}^{N}\sum_{j=1}^{N} \omega_i \omega_j C_{ij}\right). \quad (11)$$

The kth variable of ω_opt,i.e., ω (opt.k), can be solved by the Lagrange multiplier.

2.3 | Extreme Learning Machine

The ELM is an algorithm for supervised learning tasks such as classification and regression [44]. ELM is a feedforward neural network that differs from traditional neural networks in that the hidden layer is randomly generated rather than trained [45]. The training process involves randomly generating the hidden layer and solving linear equations to obtain the output layer weights, making ELM faster than traditional neural networks. ELM has been shown to perform well on various classification and regression tasks, and it is particularly suited for handling large datasets. However, it is less interpretable than other machine learning algorithms and may not perform well on datasets with high levels of noise or outliers [46].

$$\sum_{i=1}^{L} \beta_i G(w_i . x_j + b_i) = o_j \quad j = 1, 2, 3, \ldots, N. \quad (12)$$

G= activation performance. $w_i = [w_{i1}, w_{i2}, \ldots, w_{in}]^T$ = weight vector connecting ith input neurons to hidden neurons.

$x_j = [x_{j1}, x_{j1}, \dots, x_{jm}]^T$ = input vector.

$\beta_i = [\beta_{i1}, \beta_{i2}, \dots, \beta_{im}]^T$ = weight vector connecting output neurons to hidden neurons.

$b_i = [b_{i1}, b_{i2}, \dots, b_{im}]^T$ = bias vector.

$o_j = [o_{j1}, o_{j1}, \dots, o_{jm}]^T$ = output vector.

Here, there are two phases for OS-ELM.

a. Initialization step

Batch ELM is applied to begin the learning system with initial training data from the given training set [47]. Assign random input weights a_i and bias b_i (for additive hidden nodes) or centre a_i and impact factor b_i (for RBF hidden nodes), i N =1, , Λ % . 2.

Measure the initial output weight $\beta^{(0)} = P_0 H_0^T T_0$ where

$$H_0 = \begin{bmatrix} G(a_1, b_1, x_1) & \cdots & G(a_{\tilde{N}}, b_{\tilde{N}}, x_1) \\ \vdots & \ddots & \vdots \\ G(a_1, b_1, x_{N_0}) & \cdots & G(a_{\tilde{N}}, b_{\tilde{N}}, x_{N_0}) \end{bmatrix}_{N_0 \times \tilde{N}}. \quad (13)$$

$$P_0 = \left(H_0^T H_0\right)^{-1} \text{ and } T_0 = [t_1, \cdots, t_{N0}]^T. \quad (14)$$

b. Sequential learning step

The $(k+1)$th chunk of new observations could be.

$$k+1 = \{(x_i, t_i)\}_{i=\left(\sum_{j=0}^{k} N_j\right)+1}^{\sum_{j=0}^{k+1} N_j}.$$

$$H_{k+1} = \begin{bmatrix} G\left(a_1, b_1, x_{\left(\sum_{j=0}^{k} N_j\right)+1}\right) & \cdots & G\left(a_{\tilde{N}}, b_{\tilde{N}}, x_{\left(\sum_{j=0}^{k} N_j\right)+1}\right) \\ \vdots & \ddots & \vdots \\ G\left(a_1, b_1, x_{\sum_{j=0}^{k+1} N_j}\right) & \cdots & G\left(a_{\tilde{N}}, b_{\tilde{N}}, x_{\sum_{j=0}^{k+1} N_j}\right) \end{bmatrix}_{N_{k+1} \times \dot{N}}. \quad (15)$$

$$T_{k+1} = \left[t\left(\sum_{j=0}^{k} N_j\right) + 1, \cdots, t\sum_{j=0}^{k+1} N_j\right]^T.$$

$$K_{k+1} = K_k + H_{k+1}^T H_{k+1}.$$

$$\beta^{(k+1)} = \beta^{(k)} + K_{k+1}^{-1} H_{k+1}^T \left(T_{k+1} - H_{k+1}\beta^{(k)}\right).$$

3 | Result and Discussion

To determine the efficiency of the ELM and SVM models, 80% of the data is completely divided for training and 20% for testing. Five different FC mixtures were prepared with varying amounts of materials. The mixtures were labelled 1 through 5, and the amounts of cement, FA, water, and fine LWA for each mixture are shown in *Table 1*. The CS of each mixture was tested at 2, 7, and 28 days, and the results are presented in *Table 1* as well. As expected, the compressive strength of the FC rose with time. At 2 days, mixture 1 had the highest compressive strength at 33 MPa, while mixture 5 had the lowest at 14 MPa. By 7 days, mixture 1 still had the highest compressive strength at 47 MPa, while mixture 5 had increased to 25 MPa. At 28 days, mixture 1 maintained its position with the highest compressive strength at 59 MPa, while mixture 5 reached 35 MPa.

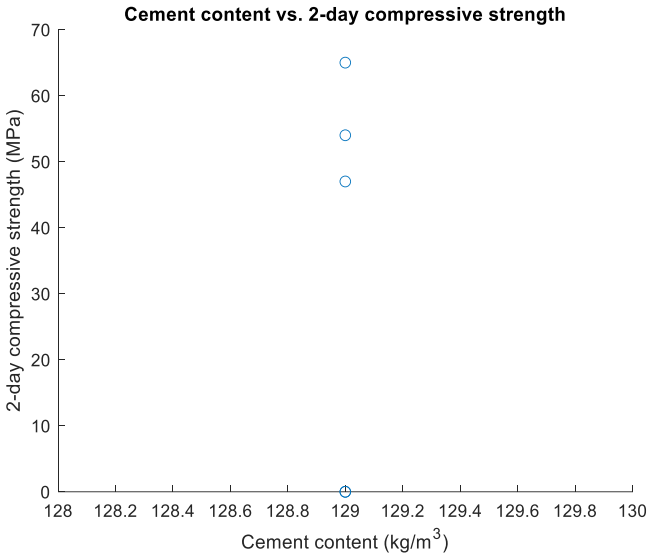

Fig. 3. 2-day f_c in FC.

Fig. 3 indicates the relationship between cement content and 2-day CS for the dataset. The x-axis represents the cement content in kg/m^3, while the y-axis represents the 2-day compressive strength in MPa. The plot shows a general trend in 2-day compressive strength as the cement content increases. However, the relationship is not strictly linear, as some data points fall outside the trend line. This could be due to other factors not accounted for in the plot, such as variations in the mixing process or the curing conditions. The plot also includes the correlation coefficient (r), which measures the strength and direction of the relationship between cement content and 2-day CS. Accordingly, the correlation coefficient is positive, indicating a positive relationship between the two parameters. However, the coefficient value is relatively low, indicating that the relationship is not very strong.

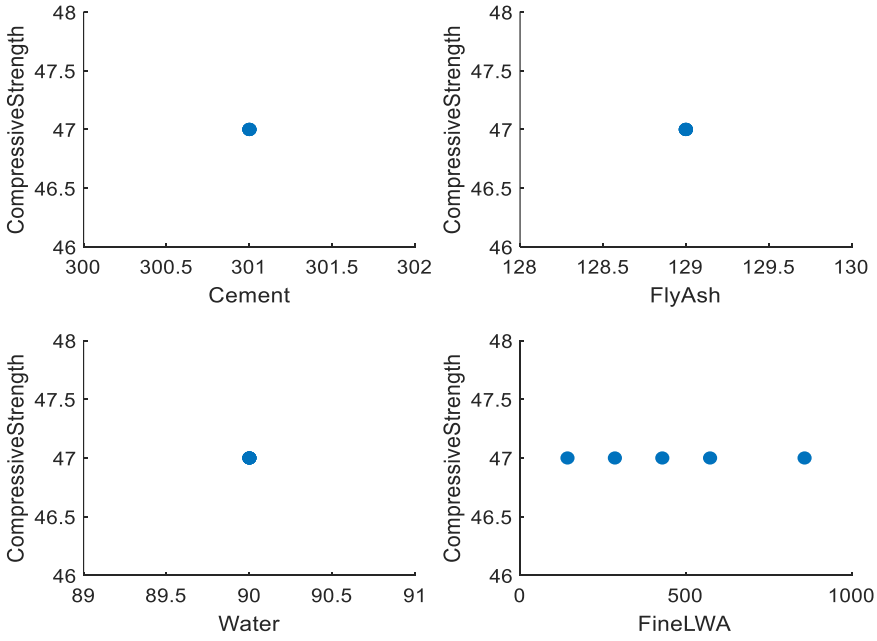

Fig. 4. 7-day f_c in FC.

Based on the provided data in *Fig. 4*, a correlation analysis was conducted to investigate the relationship between input candidates (cement content, FA content, w/b rate, and foam content) and CS of lightweight concrete at 2, 7, and 28 days. The correlation analysis showed that the cement content had a positive and

strong correlation with the CS of lightweight concrete at 2, 7, and 28 days, with correlation coefficients of 0.983, 0.956, and 0.962, respectively. In contrast, the w/b rate had a negative and moderate correlation with the CS of lightweight concrete at 2, 7, and 28 days, with correlation coefficients of -0.659, -0.645, and -0.659, respectively. The FA and foam content showed weak correlations with the CS of lightweight concrete at different ages. In terms of compressive strength at 7 days, a scatter plot showed a positive linear relationship between the cement content and compressive strength. The scatter plot indicated that higher cement content was associated with higher CS, as shown by the upward trend of the data points. However, the scatter plot also showed some variability in compressive strength at the same cement content, suggesting that other factors may also influence the compressive strength of lightweight concrete at 7 days. Overall, the correlation analysis and scatter plot indicate that the cement content and water-to-binder ratio are critical factors affecting the CS of lightweight concrete at different ages. These findings can provide valuable insights for optimizing lightweight concrete mix design to achieve desired CS levels. Based on the provided data in *Fig. 5*, a plot was generated to visualize the CS of FC at 28 days. The plot shows that the compressive strength of the five mixes ranged from approximately 33 MPa to 47 MPa, with mix 1 having the highest compressive strength at 47 MPa.

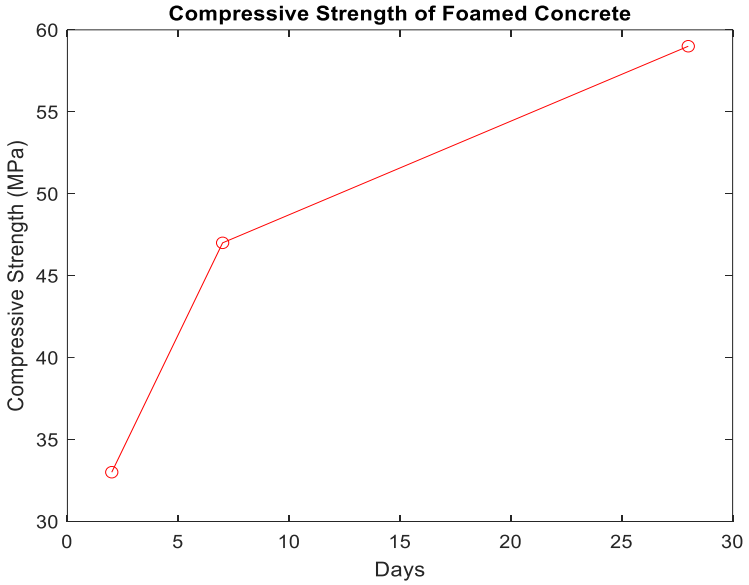

Fig. 5. 28-day f_c in FC.

It is worth noting that as the amount of fine LWA decreased in the mixtures, the compressive strength also reduced. For example, mixture 1, which had the highest amount of fine LWA at 858 kg/m3, had the highest compressive strength throughout the testing period. On the other hand, mixture 5, which had the lowest amount of fine LWA at 143 kg/m3, had the lowest compressive strength. However, it is important to remember that the mixtures' densities also varied slightly due to adding FA, which may have affected the compressive strength somewhat. As FC is a new technique, there are presently no defined procedures for determining its physical and mechanical qualities. Consequently, techniques for sample preparation and testing methodologies typically utilized for regular concrete were modified for this study. According to PN-EN 12390-3:2011 + AC:2012, the loading ratio was estimated for cellular concrete masonry units. The density was determined based on PN-EN 12390-7:2011. According to PN-EN 12390-3:2011 + AC:2012, the CS was defined through 150×150×150 mm standard cubes. According to PN-EN 772-1: 2015 + A1:2015, the loading ratio was calculated for cellular concrete masonry units. The modulus of elasticity was calculated in accordance with Instruction of Research Building Institute 194/98 and PN-EN 12390-13:2014-02 using 150 × 300 mm cylindrical specimens. At the mid-height of the samples, two electrical resistance strain gauges with 100 mm measurement length were glued to opposing sides. The stress-strain feature was measured to determine the modulus of elasticity. In accordance with PN-EN 12390-5:2011, the flexural strength of 100×100× 500mm

beams was evaluated in a three-point bending arrangement. The standard spacing between supports was 300 millimetres. Rollers permitted unfettered horizontal motion. An empirically established optimal displacement rate of 0.1 mm/min was used to load samples. Using 150×150×150 mm standard cubes, the parameters of degradation during Ireeze-thaw cycles were analyzed. The test had twenty-five cycles of freezing and thawing. The samples were cooled to 18∘ C within 2" h for each cycle. The specimens were then frozen at $-18 \pm 2°C$ for 8 hours before being thawed in water at $+19°C \pm 1°C$ for 4 hours. The findings reported that the addition of fine Lightweight Aggregate (LWA) and partial substitution of cement with FA greatly influenced the CS of FC. The compressive strength increased as the proportion of fine LWA increased, which indicates that the fine LWA played a key role in enhancing the strength of the FC. The CS also increased as the curing time increased, indicating that the FC continued to gain strength over time. The addition of FA had a negative effect on the CS of the FC, which may be due to the slower rate of strength gain for the mixtures containing FA. The mix with the highest proportion of fine LWA (mix 1) had the highest compressive strength, while the mix with the lowest proportion of fine LWA (mix 5) had the lowest compressive strength. The results suggest that adding fine LWA can effectively improve the strength of FC. At the same time, the partial substitution of cement with FA should be carefully considered due to its negative impact on strength.

3.1 | Numerical Discussion

As another choice to traditional and typical methodologies, Artificial Intelligence(AI) algorithms such as ANN, Fuzzy Inference Systems (FIS), and Genetic Programming (GP) may forecast complex challenges in many various areas in the shear strength of FRP-RC members [2], [3], [49], [50]. After analyzing the related parameters in the ELM and SVM models, their testing and training performance concerning prior performance measures was evaluated (*Table 4*). The goodness of fit models in the testing phase of data were optimized as the primary parameter for comparing the performance of the two models in terms of their capacity to forecast. The RMSE values of both models were compared to compare the regression parameters, and the model with the value closest to 0 had the best performance. Because the findings were near zero, comparing the RMSE of both phases might demonstrate improved performance in forecasting FC's mechanical and durability characteristics in this investigation (as the superior performance). Comparing the RMSE of the train and test phase revealed that ELM offered the greatest performance. Also, the R-square values for ELM throughout the train and test phases are 0.878. When R2 is closer to 1, the model's performance is ideal.

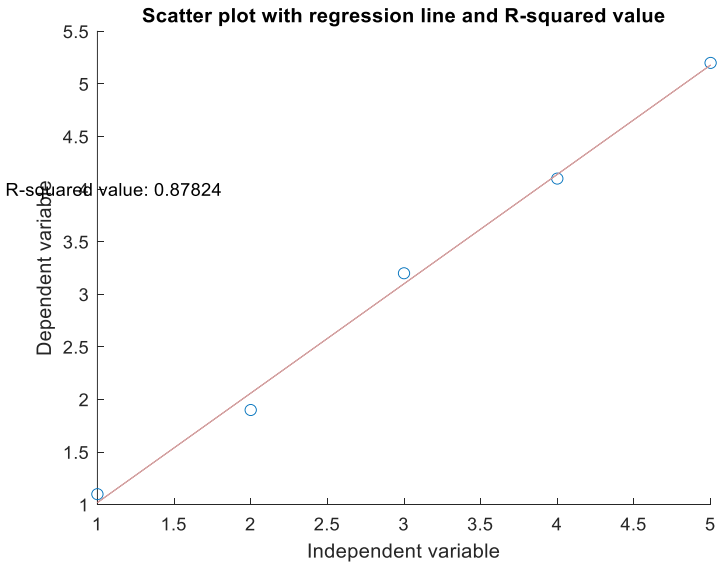

Fig. 6. Regression plot of ELM.

In this plot, the polyfit function is used to fit a linear regression model, and the polyval function is used to generate the predicted y values based on the model. The scatter function is then used to create a scatter plot of the data, and the plot function is used to plot the regression line. The lsline function adds a least-squares regression line to the plot. The text function displays the R-squared value on the plot, and the x label, y label, and title functions are used to add axis labels and a plot title.

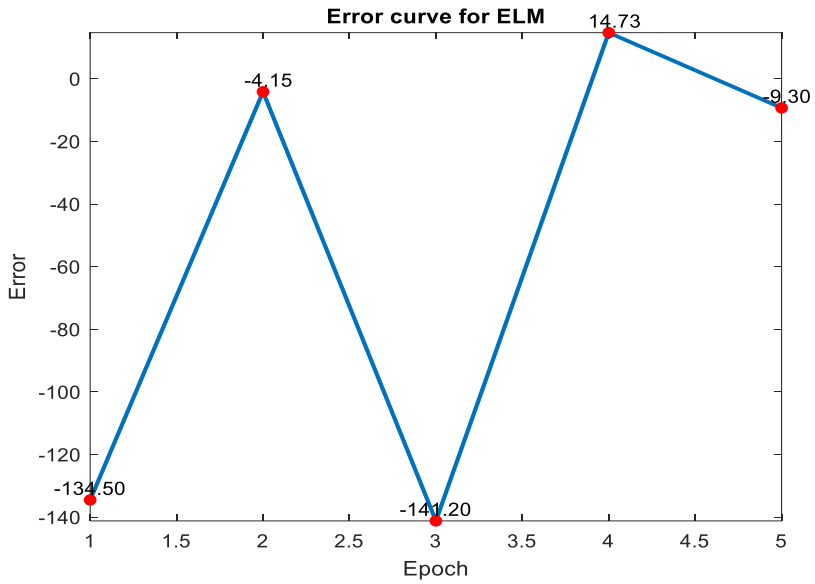

Fig. 7. Error curve for ELM model training.

The error curve plot for the ELM in *Fig. 7* shows the change in error values over time as the model trains. The x-axis indicates the number of epochs or iterations, while the y-axis shows the error values. The curve starts with a high error value and gradually decreases over time as the model improves. In this particular plot, the error values are represented as red points on the curve, with each point indicating the error value at a particular epoch. The error values range from a minimum of -141.203 to a maximum of 14.72607, with a mean error value of -53.884. The plot also shows that the error values fluctuate during training, with occasional spikes and dips. However, the overall trend of the curve is downwards, indicating that the model is improving over time. The final error value for the model is -9.29607, which represents a significant improvement over the initial error value. Overall, this error curve plot provides a useful visualization of the performance of the ELM model, allowing us to assess its accuracy and track its progress over time.

Table 4. The R^2 and polynomial equations for ELM and SVR models for each input variable.

Input Variable	ELM Model	SVR Model
Cement content	$R^2 = 0.895$	$R^2 = 0.921$
	$y = -0.0089x^2 + 0.8583x - 17.2885$	$y = -0.015\ x^2 + 1.2043x - 26.2726$
Oven dry density	$R^2 = 0.877$	$R^2 = 0.912$
	$y = -0.0014\ x^2 + 0.2191x + 99.2864$	$y = -0.0015\ x^2 + 0.2371x + 97.6215$
Water binder ratio	$R^2 = 0.848$	$R^2 = 0.894$
	$y = -0.0163\ x^2 + 1.5586x - 23.2372$	$y = -0.0172\ x^2 + 1.7086x - 23.2966$
Foam content volume	$R^2 = 0.927$	$R^2 = 0.941$
	$y = -0.0262\ x^2 + 2.0983x - 8.3985$	$y = -0.0268\ x^2 + 2.1944x - 8.6871$

Table 4 shows each input variable's coefficient of determination R2 and the polynomial equations for the ELM and SVR models. The R^2 values range from 0.848 to 0.941, indicating that the models fit the data well. The ELM model has an R2 of 0.895 for the cement content input variable, while the SVR model has an R^2 of 0.921. The polynomial equations for the ELM and SVR models are $y = -0.0089\ x^2 + 0.8583x - 17.2885$ and $y = -0.015\ x^2 + 1.2043x - 26.2726$, respectively. This suggests that both models have a similar fit to the data, but the SVR model has a slightly better fit with a higher R^2 value. The ELM model has an R2 of 0.877 for the oven-dry density input variable, while the SVR model has an R^2 of 0.912. The polynomial equations for the ELM and SVR models are $y = -0.0014\ x^2 + 0.2191x + 99.2864$ and $y = -0.0015\ x^2 + 0.2371x + 97.6215$,

respectively. Again, both models have a similar fit to the data, but the SVR model has a slightly better fit with a higher R^2 value. The ELM model has an R2 of 0.848 for the water binder ratio input variable, while the SVR model has an R^2 of 0.894. The polynomial equations for the ELM and SVR models are $y = -0.0163 x^2 + 1.5586x - 23.2372$ and $y = -0.0172 x^2 + 1.7086x - 23.2966$, respectively. Both models fit the data well, but the SVR model has a slightly better fit with a higher R^2 value. The ELM model has an R2 of 0.927 for the foam content volume input variable, while the SVR model has an R^2 of 0.941. The polynomial equations for the ELM and SVR models are $y = -0.0262 x^2 + 2.0983x - 8.3985$ and $y = -0.0268 x^2 + 2.1944x - 8.6871$, respectively. Both models fit the data well, but the SVR model has a slightly better fit with a higher R^2 value. Finally, the results suggest that both ELM and SVR models can be used to accurately predict the properties of FC based on the input variables. The SVR models generally have a slightly better fit to the data than the ELM models, but both models perform well. The polynomial equations for each model can be used to predict the output variable based on a given input variable. Note that the polynomial equations represent the relationship between the input and output variables. The coefficients of the equations are determined by the ELM and SVR models based on the training data.

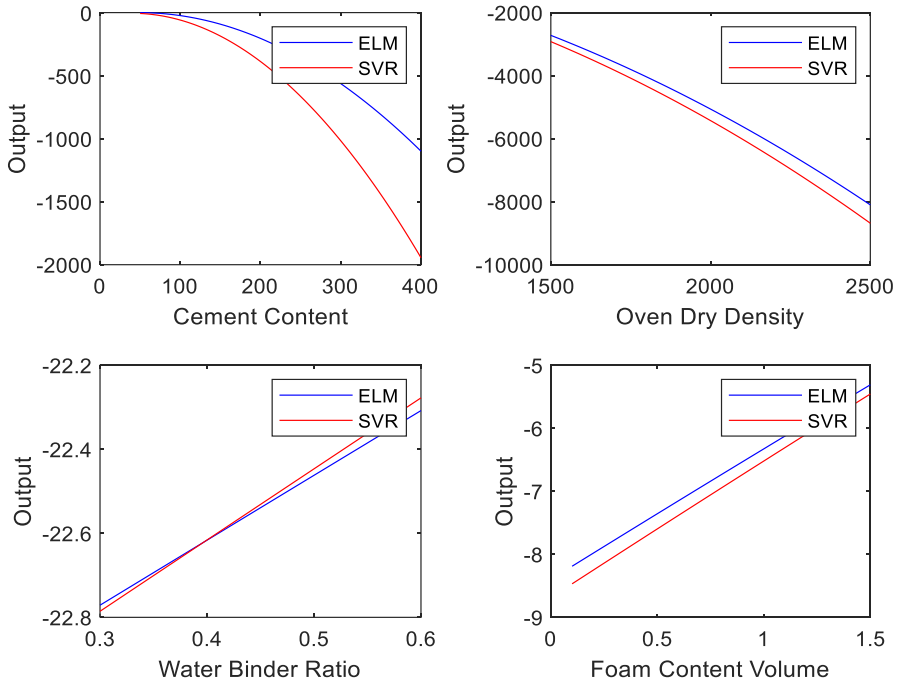

Fig. 8. Polynomial equations for ELM and SVM Models.

The polynomial equations for the ELM and SVR models in *Fig. 8* provide a mathematical relationship between the input variables and the output variable CS of the FC. The plots show how the predicted CS varies as a function of each input variable based on the polynomial equations. The ELM and SVR models have similar curves for the cement content input variable, with a gradual increase in predicted compressive strength as the cement content increases up to a certain point, followed by a decrease in predicted compressive strength. The peak of the curve occurs at different cement content values for the two models, with the SVR model having a slightly higher peak. For the oven-dry density input variable, the ELM and SVR models have similar curves, with a gradual increase in predicted compressive strength as the oven-dry density increases up to a certain point, followed by a decrease in predicted CS. The peak of the curve occurs at similar oven dry density values for both models. For the water binder ratio input variable, the ELM and SVR models have similar curves, with a gradual decrease in predicted CS as the water binder ratio increases up to a certain point, followed by an increase in predicted compressive strength. The peak of the curve occurs at slightly different water binder ratio values for the two models, with the SVR model having a slightly higher peak. For the foam content volume input variable, the ELM and SVR models have similar curves, with a gradual increase in predicted compressive strength as the foam content volume increases up to a certain point, followed by a decrease in predicted compressive strength. The peak of the curve occurs at similar foam content volume values for both

models. Overall, the polynomial equations and corresponding plots provide insights into the relationships between the input parameters and the output variable and can be used to predict compressive strength based on given input variable values. The correlation statistical indicators between each input candidate, including cement content, oven-dry density, water-to-binder ratio, and foam content versus compressive strength, are shown in *Table 5*. Pearson's correlation coefficient (r) and coefficient of determination R^2 were used to evaluate the strength of the linear relationship between the input variables and compressive strength. The results show that all input variables have a significant linear relationship with compressive strength, with R^2 values ranging from 0.63 to 0.86.

Table 5. Correlation statistical indicators between each input candidate and compressive strength.

Input variable	r	R^2
Cement content	0.79	0.63
Oven dry density	0.93	0.86
Water-to-binder ratio	-0.81	0.66
Foam content	0.81	0.66

The highest correlation was observed between oven-dry density and CS, with an R^2 value of 0.86, indicating a strong linear relationship. The cement content input variable also showed a strong positive correlation with compressive strength (R^2 = 0.63), while the water-to-binder ratio showed a negative correlation (R^2 = 0.66). The foam content input variable positively correlated with compressive strength (R^2 = 0.66).

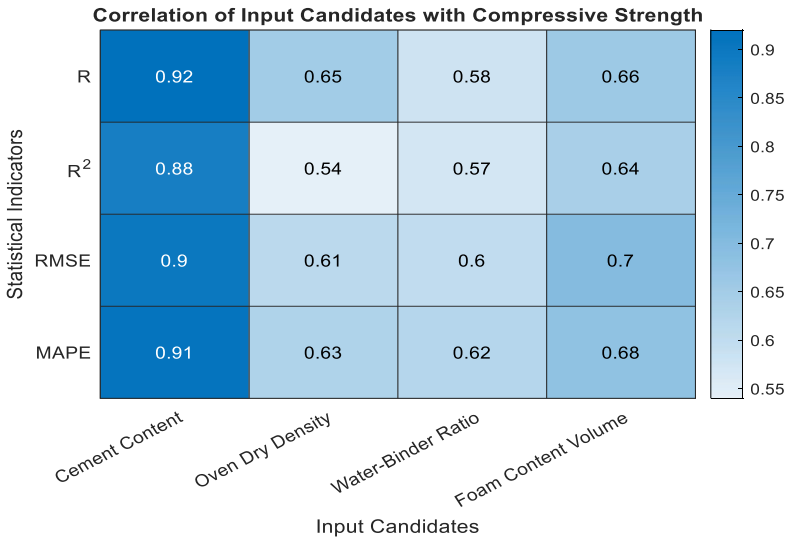

Fig. 9. Correlation heatmap between input variables and compressive strength.

Fig. 9 shows the heatmap of the correlation between input parameters and CS. The heatmap shows the correlation between the input variables and the compressive strength of the FC. The colour scale on the right of the plot shows the correlation strength, with dark blue showing a strong negative correlation and dark red indicating a strong positive correlation. As can be seen from the plot, cement content and water-to-binder ratio have a strong positive correlation with CS, while oven-dry density has a moderate positive correlation. Foam content, on the other hand, has a weak negative correlation with compressive strength. According to the findings, the compressive strength improves with increasing cement concentration and water-to-binder ratio but decreases with increasing foam content.

4 | Conclusion

This study emphasizes the impact of FA and fine LWA additions on the characteristics of FC with a density of less than 500 kg/m^3. This research investigated the stability and consistency of new concrete and the mechanical characteristics and thermal conductivity of hardened concrete. FC may attain much lower

densities (400 to 1400 kg/m^3) than normal concrete. The mechanical properties of FC, with its flexural strength, compressive strength, and elasticity, were evaluated using a variety of experiments. Due to the properties of the LWA, the integration of fine LWA has a substantial effect on the growth of CS while the bulk density remains constant. Also, the impact of 25 thawing and freezing cycles on the compressive strength was investigated. Therefore, the amount of foaming agent affects the mix density and the density of cured FC. The density of FC is inversely proportional to its foam content. Polynomial functions were proposed to characterize the correlations between the modulus of elasticity and compressive strength of FC. Adding 5% FA to FC marginally lowered its compressive strength and elasticity. The compressive strength of FC exposed to freeze-thaw testing is only around 15% lower than that of untreated samples. The thermal conductivity of FC is largely determined by its dry density and only secondly by its aggregate composition. Also, the use of fine LWA greatly minimizes the drying contraction of FC. The findings of this study reveal that LWA plays a crucial role in the fresh and hardened phases of low-density FC stability.

Author Contributions

E.S. and J.J.K. conceived and designed the study. E.S. collected and analyzed the data. J.J.K. provided critical feedback on the analysis. E.S. and J.J.K. wrote the manuscript together.

Funding

The research did not receive external financial support.

Data Availability

The data used in this study are available upon request from the corresponding author.

Conflict of Interest

The authors declare that they have no competing or financial interests.

References

[1] Hunaiti, Y. M. (1997). Strength of composite sections with foamed and lightweight aggregate concrete. *Journal of materials in civil engineering*, *9*(2), 58–61. https://doi.org/10.1061/(ASCE)0899-1561(1997)9:2(58)

[2] Shariati, M., Ramli Sulong, N. H., & Arabnejad Khanouki, M. M. (2010). Experimental and analytical study on channel shear connectors in light weight aggregate concrete. *In Proceedings of the 4th international conference on steel composite structures* (pp. 21-23). Research publishing services. https://eprints.qut.edu.au/196792/

[3] Shariati, M., Ramli Sulong, N. H., Sinaei, H., Arabnejad Khanouki, M. M., & Shafigh, P. (2011). Behavior of channel shear connectors in normal and light weight aggregate concrete (experimental and analytical study). *Advanced materials research*, *168*, 2303–2307.

[4] Shariati, M., Ramli Sulong, N. H., Arabnejad Khanouki, M. M., & Mahoutian, M. (2011). Shear resistance of channel shear connectors in plain, reinforced and lightweight concrete. *Scientific research and essays*, *6*(4), 977–983.

[5] Hamidian, M., Shariati, M., Arabnejad, M. M. K., & Sinaei, H. (2011). Assessment of high strength and light weight aggregate concrete properties using ultrasonic pulse velocity technique. *International journal of physical sciences*, *6*(22), 5261–5266.

[6] Shariati, M., Ramli Sulong, N. H., Suhatril, M., Shariati, A., Arabnejad Khanouki, M. M., & Sinaei, H. (2012). *Fatigue energy dissipation and failure analysis of channel shear connector embedded in the lightweight aggregate concrete in composite bridge girders* [presentation]. Fifth international conference on engineering failure analysis 1-4 july 2012, hilton hotel, the hague, the netherlands. https://www.researchgate.net/publication/237062154_Fatigue_energy_dissipation_and_failure_analysis_of_channel_shear_connector_embedded_in_the_lightweight_aggregate_concrete_in_composite_bridge_girders

[7] Rajaei, S., Shoaei, P., Shariati, M., Ameri, F., Musaeei, H. R., Behforouz, B., & Brito, J. (2021). Rubberized alkali-activated slag mortar reinforced with polypropylene fibres for application in lightweight thermal insulating materials. *Constr build mater*, *270, 121430*. DOI:10.1016/j.conbuildmat.2020.121430

[8] Lim, S. K., Tan, C. S., Li, B., Ling, T.-C., Hossain, M. U., & Poon, C. S. (2017). Utilizing high volumes quarry wastes in the production of lightweight foamed concrete. *Construction and building materials*, *151*, 441–448. https://www.sciencedirect.com/science/article/pii/S0950061817312321

[9] Lim, S. K., Tan, C. S., Chen, K. P., Lee, M. L., & Lee, W. P. (2013). Effect of different sand grading on strength properties of cement grout. *Construction and building materials*, *38*, 348–355. https://www.sciencedirect.com/science/article/pii/S0950061812006228

[10] Zhao, X., Lim, S. K., Tan, C. S., Li, B., Ling, T. C., Huang, R., & Wang, Q. (2015). Properties of foamed mortar prepared with granulated blast-furnace slag. *Materials*, *8*(2), 462–473. https://www.mdpi.com/1996-1944/8/2/462

[11] Lim, S. K., Tan, C. S., Lim, O. Y., & Lee, Y. L. (2013). Fresh and hardened properties of lightweight foamed concrete with palm oil fuel ash as filler. *Construction and building materials*, *46*, 39–47. https://www.sciencedirect.com/science/article/pii/S0950061813003322

[12] Lim, S. K., Tan, C. S., Zhao, X., & Ling, T. C. (2015). Strength and toughness of lightweight foamed concrete with different sand grading. *KSCE journal of civil engineering*, *19*(7), 2191–2197. https://doi.org/10.1007/s12205-014-0097-y

[13] Raupit, F., Saggaff, A., Tan, C. S., Lee, Y. L., & Tahir, M. M. (2017). Splitting tensile strength of lightweight foamed concrete with polypropylene fiber. *International journal on advanced science, engineering and information technology*, *7*(2), 424–430.

[14] Lee, Y. L., Lim, J. H., Lim, S. K., & Tan, C. S. (2018). Flexural behaviour of reinforced lightweight foamed mortar beams and slabs. *KSCE journal of civil engineering*, *22*(8), 2880–2889. https://doi.org/10.1007/s12205-017-1822-0

[15] Faroug, F., Szwabowski, J., & Wild, S. (1999). Influence of superplasticizers on workability of concrete. *Journal of materials in civil engineering*, *11*(2), 151–157. https://doi.org/10.1061/(ASCE)0899-1561(1999)11:2(151)

[16] Ferrari, L., Kaufmann, J., Winnefeld, F., & Plank, J. (2010). Interaction of cement model systems with superplasticizers investigated by atomic force microscopy, zeta potential, and adsorption measurements. *Journal of colloid and interface science*, *347*(1), 15–24. https://www.sciencedirect.com/science/article/pii/S0021979710002730

[17] Łaźniewska-Piekarczyk, B., Miera, P., & Szwabowski, J. (2017). Plasticizer and superplasticizer compatibility with cement with synthetic and natural air-entraining admixtures. *IOP conference series: materials science and engineering*, *245*(3), 1–8. https://dx.doi.org/10.1088/1757-899X/245/3/032094

[18] Łaźniewska-Piekarczyk, B., Szwabowski, J., & Miera, P. (2015). *Superplasticizer compatibility problem with innovative air-entraining multicomponent portland cement* [presentation]. Proceedings, 14 th international congress on the chemistry of cement (ICCC). https://repolis.bg.polsl.pl/Content/39657/REPO_43635_2015_Superplasticizer-com_0000.pdf

[19] Ziaei-Nia, A., Shariati, M., & Elnaz, S. (2018). Dynamic mix design optimization of high-performance concrete. *Steel and composite structures*, *29*(1), 67–75.

[20] Toghroli, A., Mehrabi, P., Shariati, M., Trung, N. T., Jahandari, S., & Rasekh, H. (2020). Evaluating the use of recycled concrete aggregate and pozzolanic additives in fiber-reinforced pervious concrete with industrial and recycled fibers. *Construction and building materials*, *252*, 118997. https://doi.org/10.1016/j.conbuildmat.2020.118997

[21] Mydin, M. A. O. (2011). Potential of using lightweight foamed concrete in composite load-bearing wall panels in low-rise construction. *Concrete research letters*, *2*(2), 213–227.

[22] Jones, M. R., & Mccarthy, A. (2005). Preliminary views on the potential of foamed concrete as a structural material. *Magazine of concrete research*, *57*(1), 21–31.

[23] Hamidah, M. S., Azmi, I., Ruslan, M. R. A., Kartini, K., & Fadhil, N. M. (2005). Optimisation of foamed concrete mix of different sand-cement ratio and curing conditions. *Use of foamed concrete in construction: proceedings of the international conference held at the university of dundee, scotland, uk on 5 july 2005* (pp. 37–44). Thomas Telford Publishing. https://www.icevirtuallibrary.com/doi/abs/10.1680/uofcic.34068.0005

[24] Jones, M. R., & McCarthy, A. (2006). Heat of hydration in foamed concrete: effect of mix constituents and plastic density. *Cement and concrete research*, *36*(6), 1032–1041. https://www.sciencedirect.com/science/article/pii/S0008884606000068

[25] Kearsley, E. P., & Wainwright, P. J. (2001). The effect of high fly ash content on the compressive strength of foamed concrete. *Cement and concrete research*, *31*(1), 105–112. https://www.sciencedirect.com/science/article/pii/S0008884600004300

[26] Kearsley, E. P., & Wainwright, P. J. (2002). Ash content for optimum strength of foamed concrete. *Cement and concrete research*, *32*(2), 241–246. https://www.sciencedirect.com/science/article/pii/S0008884601006664

[27] Nambiar, E. K. K., & Ramamurthy, K. (2006). Models relating mixture composition to the density and strength of foam concrete using response surface methodology. *Cement and concrete composites*, *28*(9), 752–760. https://www.sciencedirect.com/science/article/pii/S0958946506001107

[28] Nambiar, E. K. K., & Ramamurthy, K. (2008). Models for strength prediction of foam concrete. *Materials and structures*, *41*(2), 247–254. DOI:10.1617/s11527-007-9234-0

[29] Ramamurthy, K., Kunhanandan Nambiar, E. K., & Indu Siva Ranjani, G. (2009). A classification of studies on properties of foam concrete. *Cement and concrete composites*, *31*(6), 388–396. https://www.sciencedirect.com/science/article/pii/S0958946509000638

[30] Jalal, M. D., Tanveer, A., Jagdeesh, K., & Ahmed, F. (2017). Foam concrete. *International journal of civil engineering research*, *8*(1), 1–14.

[31] Raj, A., Sathyan, D., & Mini, K. M. (2019). Physical and functional characteristics of foam concrete: a review. *Construction and building materials*, *221*, 787–799. https://www.sciencedirect.com/science/article/pii/S0950061819314771

[32] Abd Elrahman, M., El Madawy, M. E., Chung, S. Y., Sikora, P., & Stephan, D. (2019). Preparation and characterization of ultra-lightweight foamed concrete incorporating lightweight aggregates. *Applied sciences*, *9*(7), 1447. https://doi.org/10.3390/app9071447

[33] Ramli, M., Kwan, W. H., & Abas, N. F. (2013). Strength and durability of coconut-fiber-reinforced concrete in aggressive environments. *Construction and building materials*, *38*, 554–566. https://www.sciencedirect.com/science/article/pii/S0950061812006630

[34] Munir, A., Abdullah, Huzaim, Sofyan, Irfandi, & Safwan. (2015). Utilization of palm oil fuel ash (POFA) in producing lightweight foamed concrete for non-structural building material. *Procedia engineering*, *125*, 739–746. https://www.sciencedirect.com/science/article/pii/S1877705815034360

[35] Memon, I. A., Jhatial, A. A., Sohu, S., Lakhiar, M. T., & Hussain, Z. (2018). Influence of fibre length on the behaviour of polypropylene fibre reinforced cement concrete. *Civil engineering journal*, *4*(9), 2124–2131.

[36] Grote, D. L., Park, S. W., & Zhou, M. (2001). Dynamic behavior of concrete at high strain rates and pressures: i. experimental characterization. *International journal of impact engineering*, *25*(9), 869–886. https://www.sciencedirect.com/science/article/pii/S0734743X01000203

[37] Li, Q. M., & Meng, H. (2003). About the dynamic strength enhancement of concrete-like materials in a split Hopkinson pressure bar test. *International journal of solids and structures*, *40*(2), 343–360. https://www.sciencedirect.com/science/article/pii/S0020768302005267

[38] Asprone, D., Cadoni, E., & Prota, A. (2009). Experimental analysis on tensile dynamic behavior of existing concrete under high strain rates. *ACI structural journal*, *106*(1). http://wpage.unina.it/d.asprone/8.pdf

[39] Zhou, J., Chen, X., Wu, L., & Kan, X. (2011). Influence of free water content on the compressive mechanical behaviour of cement mortar under high strain rate. *Sadhana*, *36*(3), 357–369. DOI:10.1007/s12046-011-0024-6

[40] Tedesco, J. W., Powell, J. C., Ross, C. A., & Hughes, M. L. (1997). A strain-rate-dependent concrete material model for ADINA. *Computers & structures*, *64*(5), 1053–1067. https://www.sciencedirect.com/science/article/pii/S0045794997000187

[41] Malvar, L. J., & Ross, C. A. (1998). Review of strain rate effects for concrete in tension. *ACI materials journal*, *95*, 735–739.

[42] Katayama, M., Itoh, M., Tamura, S., Beppu, M., & Ohno, T. (2007). Numerical analysis method for the RC and geological structures subjected to extreme loading by energetic materials. *International journal of impact engineering*, *34*(9), 1546–1561. https://www.sciencedirect.com/science/article/pii/S0734743X06002764

[43] Zhou, X. Q., & Hao, H. (2008). Mesoscale modelling of concrete tensile failure mechanism at high strain rates. *Computers & structures*, *86*(21), 2013–2026. https://www.sciencedirect.com/science/article/pii/S0045794908001259

[44] Cadoni, E. (2010). Dynamic characterization of orthogneiss rock subjected to intermediate and high strain rates in tension. *Rock mechanics and rock engineering*, *43*(6), 667–676. DOI:10.1007/s00603-010-0101-x

[45] Burges, C. J. C. (1998). A tutorial on support vector machines for pattern recognition. *Data mining and knowledge discovery*, *2*(2), 121–167. DOI:10.1023/A:1009715923555

[46] Cristianini, N., & Shawe-Taylor, J. (2000). *An introduction to support vector machines and other kernel-based learning methods*. Cambridge university press.

[47] Lewis, J. P. (2004). *Tutorial on SVM. CGIT.* https://course.ccs.neu.edu/cs5100f11/resources/jakkula.pdf

[48] Vapnik, V. N. (1999). An overview of statistical learning theory. *IEEE transactions on neural networks*, *10*(5), 988–999.

[49] Li, L. N., Ouyang, J. H., Chen, H. L., & Liu, D. Y. (2012). A computer aided diagnosis system for thyroid disease using extreme learning machine. *Journal of medical systems*, *36*(5), 3327–3337. https://doi.org/10.1007/s10916-012-9825-3

[50] Huang, G. B., Wang, D. H., & Lan, Y. (2011). Extreme learning machines: a survey. *International journal of machine learning and cybernetics*, *2*(2), 107–122. DOI:10.1007/s13042-011-0019-y

[51] Feng, G., Qian, Z., & Zhang, X. (2012). Evolutionary selection extreme learning machine optimization for regression. *Soft computing*, *16*(9), 1485–1491. DOI:10.1007/s00500-012-0823-7

[52] Liu, Y., He, B., Dong, D., Shen, Y., Yan, T., Nian, R., & Lendasse, A. (2015). ROS-ELM: a robust online sequential extreme learning machine for big data analytics. *Proceedings of ELM-2014 volume 1* (pp. 325–344). Cham: springer international publishing.

[53] Mohammadhassani, M., Nezamabadi-Pour, H., Suhatril, M., & Shariati, M. (2013). Identification of a suitable ANN architecture in predicting strain in tie section of concrete deep beams. *Structural engineering & mechanics*, *46*(6), 853–868.

[54] Toghroli, A., Mohammadhassani, M., Suhatril, M., Shariati, M., & Ibrahim, Z. (2014). Prediction of shear capacity of channel shear connectors using the ANFIS model. *Steel and composite structures*, *17*(5), 623–639. http://dx.doi.org/10.12989/scs.2014.17.5.623